Bulletin of Earthquake Engineering
https://doi.org/10.1007/s10518-024-01875-3

S.I. : FEBRUARY 6, 2023, KAHRAMANMARAŞ-TÜRKIYE EARTHQUAKES

Soil liquefaction sites following the February 6, 2023, Kahramanmaraş-Türkiye earthquake sequence

Kemal Onder Cetin[1,2] · Berkan Soylemez[1] · Hayri Guzel[1] · Elife Cakir[1]

Received: 16 August 2023 / Accepted: 6 February 2024

Abstract
Seismically induced soil liquefaction was listed as one of the major causes of damage observed in the natural and built environment during the 2023 Türkiye-Kahramanmaraş earthquake sequence. Reconnaissance field investigations were performed to collect perishable data and document the extent of damage immediately after the events. The sites with surface manifestations of seismic soil liquefaction in the form of soil ejecta, excessive foundation and ground deformations were identified and documented. The deformations were mapped, and samples from ejecta were retrieved. The ejecta samples were predominantly classified as sands with varying degrees of fines. Laboratory test results performed on liquefied soil ejecta revealed that the fines-containing liquefied ejecta samples are mostly classified as low plasticity clays (CL). Most of CL soil type ejecta were retrieved from Gölbaşı–Adıyaman region. The liquid limits of these samples varied in between 32 and 38%, their plasticity index values were estimated in the range of 16–23%. Surprisingly, two ejecta samples with plasticity indices higher than 30% were retrieved from Hatay airport, one of which was classified as high plasticity clay (CH). The majority of the fine-grained ejecta samples fall either on "Zone B: Testing Recommended" region of the Seed et al. (Keynote presentation, 26th Annual ASCE Los Angeles Geotechnical Spring Seminar, Long Beach, CA, 2003) susceptibility chart. Moreover, 12 out of 74 samples fall outside the susceptible limits defined by Seed et. These preliminary results suggest that clayey soils can produce liquefied ejecta when subjected to cyclic loading. Detailed site investigation and laboratory testing programs are ongoing to further investigate this rather unexpected response. Until their findings become available, the liquefaction susceptibility of silty-clayey soils' mixtures is recommended to be assessed conservatively with caution.

Keywords Liquefaction · Grain size · Atterberg limits · Low plasticity · Kahramanmaraş earthquake · Susceptibility

✉ Kemal Onder Cetin
ocetin@metu.edu.tr; kemalondercetin@gmail.com

[1] Middle East Technical University, Universiteler Mah. Dumlupınar Bulv, 06800 Cankaya-Ankara, Turkey

[2] Earthquake Engineering Research Center, Middle East Technical University, 06800 Ankara, Turkey

Published online: 18 March 2024

1 Introduction

On February 6, 2023, two earthquakes, with moment magnitudes M7.8 and M7.6, occurred in Kahramanmaraş-Türkiye on the East Anatolian Fault zone, at local times 04:17 and 13:24, respectively. After the mainshocks, more than ten thousand earthquakes were recorded in the period of February 6 to March 1, within 200 km radii from the event epicenters. Over 400 of these aftershocks have $M \geq 5.0$. Figure 1 shows the focal mechanisms and spatial distribution of mainshocks and aftershocks along with their induced fault rupture patterns. The epicenter of the first event, which has a focal depth of 8.6 km, is located at 37.288°N and 37.043°E (AFAD), close to Kahramanmaraş-Pazarcık. The second event has a focal depth of 7.0 km with its epicenter in Kahramanmaraş-Elbistan-Ekinözü, at 38.089°N, 37.239°E.

The moment tensor solution suggested purely left-lateral strike-slip during both events. The fault rupture of the first event was triggered on Narlı Fault, at the northern end of the Dead Sea Fault zone. The rupture stepped over to the East Anatolian Fault zone, and continued along Pazarcık, Erkenek, and Amanos segments, propagating bilaterally in the north- east and south-west directions. The total fault rupture length exceeded 300 km, with a maximum offset of 4 m (Cetin et al. 2023b, a; Cetin and Ilgac 2023). After the Ekinözü-Elbistan event, a 160 km long fault rupture is mapped with a maximum offset of 6 m. The second event was initiated on Çardak Fault and propagated along Doğanşehir Fault Zone.

During the first event, the maximum peak ground acceleration (PGA) levels were recorded in Hatay-Antakya, where most of the damage was reported. The PGA levels at SGMS # 3126 were recorded as 1.23 g and 1.04 g in the north–south (NS) and east-east (EW) directions, respectively. Similarly, 244 SGMS recorded the second event. The

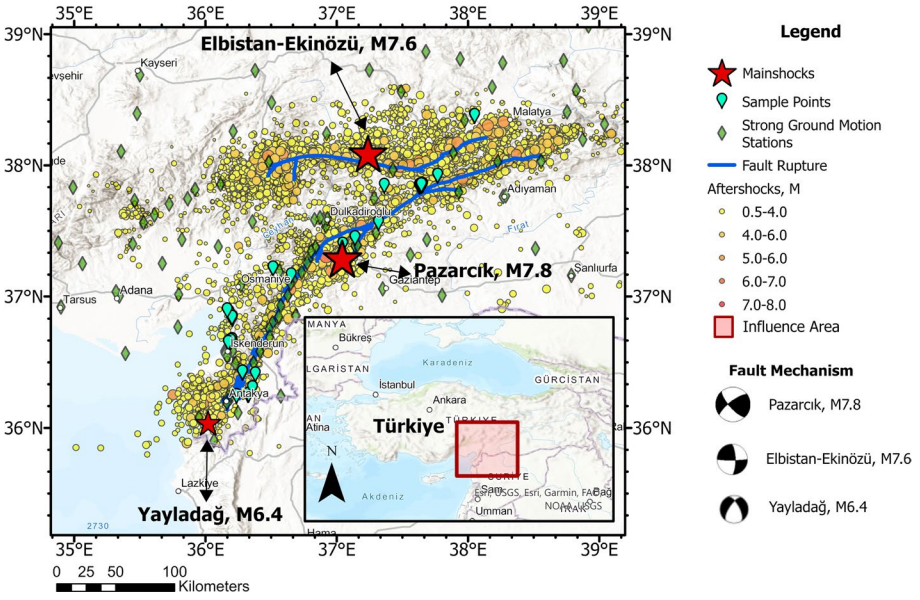

Fig. 1 The spatial distribution of mainshocks and aftershocks (as of March 1, 2023) along with the induced fault rupture patterns of Türkiye-Kahramanmaraş-Pazarcık and Ekinözü-Elbistan Earthquake sequence

maximum PGA was recorded as 0.65 and 0.53 g in the NS and EW directions, respectively, at Kahramanmaraş-Göksun Station 4612. The Ekinözü-Elbistan $M_w = 7.6$ earthquake affected the northern provinces of Kahramanmaraş, Malatya, Adıyaman, and Kayseri, the most.

After the earthquakes, reconnaissance field investigations were performed to collect perishable data and document the extent of damage to the natural and built environment. As part of these reconnaissance studies, the sites with surface manifestations of seismic soil liquefaction in the form of soil ejecta, excessive foundation and ground deformations were identified and documented. The deformations were mapped and samples from ejecta were retrieved. Within the confines of this manuscript, the liquefied soil sites are introduced first. The discussions are then followed by the presentation of the results of soil classification test, which are performed on the retrieved soil ejecta at liquefied sites. The soil classification laboratory test results are comparatively shown on the plasticity chart summarizing the Wang (1979) soil ejecta database. Similarly, liquefaction susceptibility chart recommendation by Seed et al. (2003) is used to comparatively present and assess the resulting soil ejecta database.

2 Liquefied soil sites

Reconnaissance studies to identify liquefied soil sites started on the third day after the earthquakes and continued for longer than 2 months. Various research groups contributed to the reconnaissance studies, and the resulting information is documented on a digital platform named *SiteEye* (Saha Gözü, in Turkish), which is accessible at www.sahagozu.com. A total of 428 liquefaction case history sites were identified as reported in various documents including but not limited to Cetin and Ilgac (2023), Cetin et al. (2023a), Cetin et al. (2023b), and Moug et al. (2023). A map showing the locations of liquefied sites is presented in Fig. 2.

The liquefaction case history sites were grouped in 6 geographical regions, namely L1 through L6, as presented in the same figure. A higher resolution map of these liquefaction regions is given in Figs. 3, 4 and 5. For each liquefaction region, a set of sample pictures documenting the surface manifestations of liquefaction triggering is provided in the same figures.

A sample summary of these liquefaction sites is presented in Table 1, whereas a complete presentation of them is provided in the electronic supplements. As part of the summary tables information regarding the coordinates of the site, and type of liquefaction surface manifestations in the form of soil ejecta (SE), lateral spreading (LS), excessive ground settlement (EGS), excessive foundation displacements (EFD) is provided.

3 Characteristics of liquefied soil ejecta

A total of 81 samples were retrieved from seismic soil liquefaction sites, shown in Fig. 6. The regions where these samples were retrieved are labeled as A through F. These liquefied soil ejecta samples were tested at Middle East Technical University (METU) Soil Mechanics laboratory to assess their grain size and distribution characteristics along with their consistency limits.

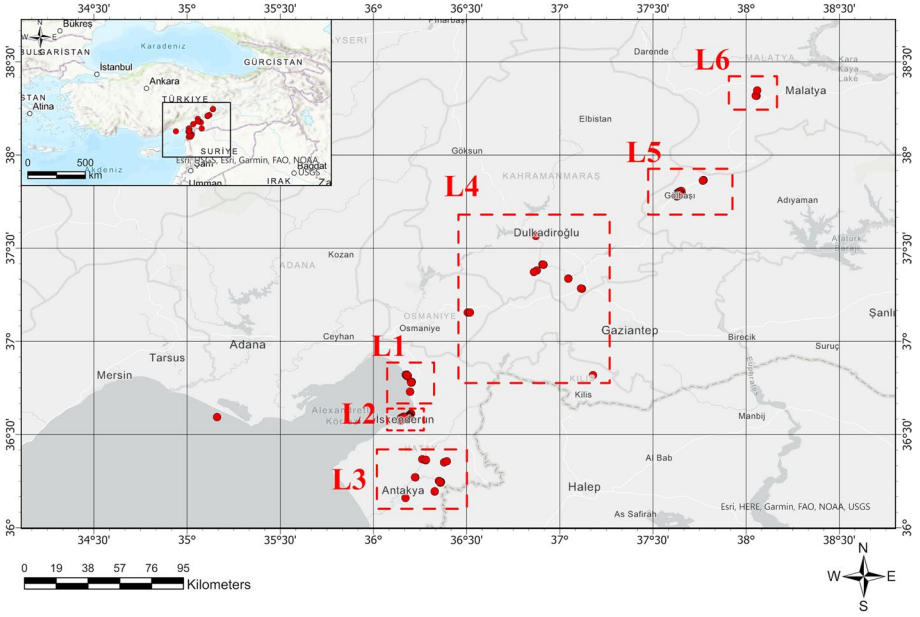

Fig. 2 Map of liquefaction case history sites

4 Sampling and testing procedures

Consistent with the extent of the area shaken by the earthquake sequence, samples were retrieved from also a wide range of locations, including but not limited to beaches, fishermen's wharf, ports, factories, schools, and residential buildings (collapsed and non-collapsed), Hatay airport, bridge abutments, dams, farmlands, etc. Similar to the soil liquefaction sites, the regions where ejecta samples were collected were clustered geographically and labeled A through F. In Fig. 7, sample pictures are presented, which show the ejecta materials retrieved from regions A through F. Each sample is assigned a sample identification number, and their grain size, distribution and consistency limit characteristics are assessed, which are summarized in the next section.

When retrieving surface soil ejecta from liquefaction sites, special attention was given to collecting representative soil samples. To achieve this, a continuous sampling approach was employed by pushing vertically a tube into the ejecta cone (or volcano). This approach was adopted to eliminate concerns related to possible segregation or layering within the ejecta material. Moreover, efforts were made to trace the travel path of the surface ejecta and identify its origin, thereby confirming that the surface ejecta accurately represented the liquefied soil layer. This confirmation was essential to ensure that the material had not eroded to the ground surface due to excess pore water pressure-induced flow. Where available, existing borelogs were utilized to support this validation process. However, in instances where site-specific borelog information was absent, attributing the characteristics of the ejecta soil sample directly to potential liquefied soil layers became challenging. To address this potential ambiguity, additional site investigations, laboratory testing and liquefaction triggering evaluations were needed for more accurate conclusions, further discussions of which is beyond the scope of this preliminary (reconnaissance) assessment manuscript.

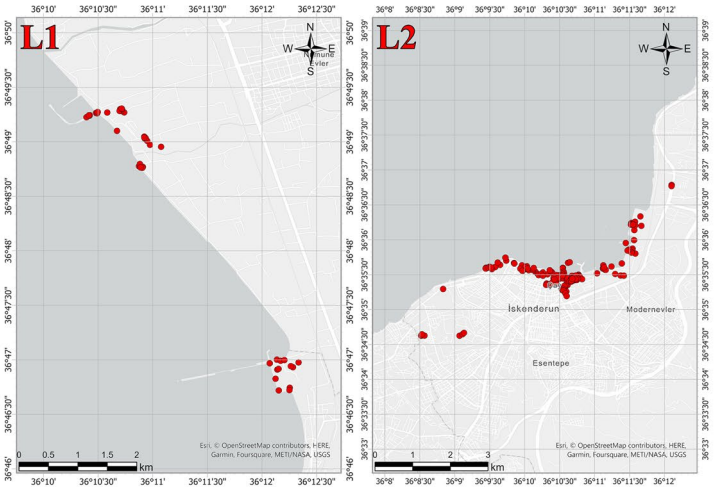

(a)

Soil ejecta
at Lat:36.7819583˚N, Long:36.20253˚E

Lateral spreading
at Lat:36.778661˚N, Long:36.202563˚E

(b)

Soil Ejecta, excessive settlement
at Lat:36.590223˚N, Long:36.177023˚E

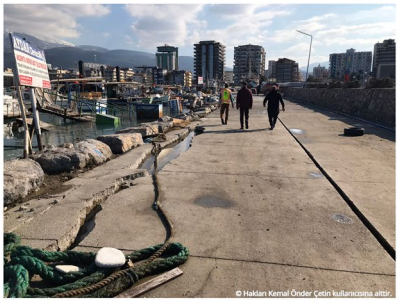

Lateral spreading, excessive settlement
at Lat:36.593308˚N, Long:36.175766˚E

(c)

Fig. 3 **a)** A higher resolution map of liquefaction regions L1 and L2, **b)** sample pictures from L1 region, and **c)** sample pictures from L2 region

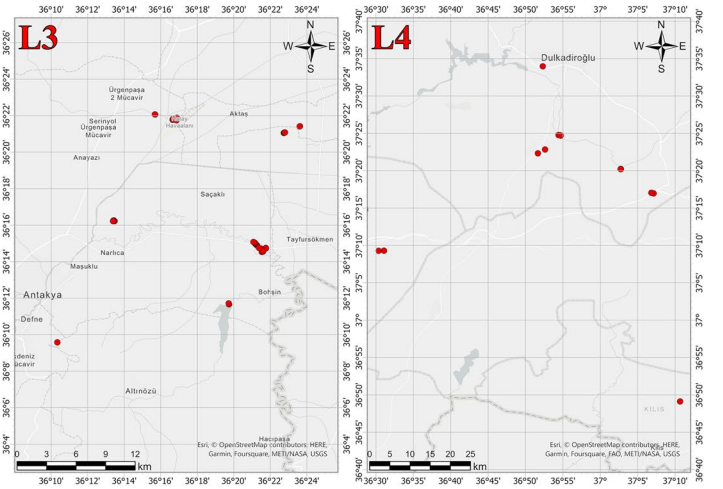

(a)

Sand volcanoes
at Lat:36.350867˚N, Long:36.379072˚E

Sand boils, lateral spreading
at Lat:36.351305˚N, Long:36.379810˚E

(b)

Sand boils
at Lat:37.337105˚N, Long:37.045719˚E

Soil ejecta
at Lat:37.86312˚N, Long:37.76752˚E

(c)

Fig. 4 **a)** A higher resolution map of liquefaction regions L3 and L4, **b)** sample pictures from L3 region, and **c**) sample pictures from L4region

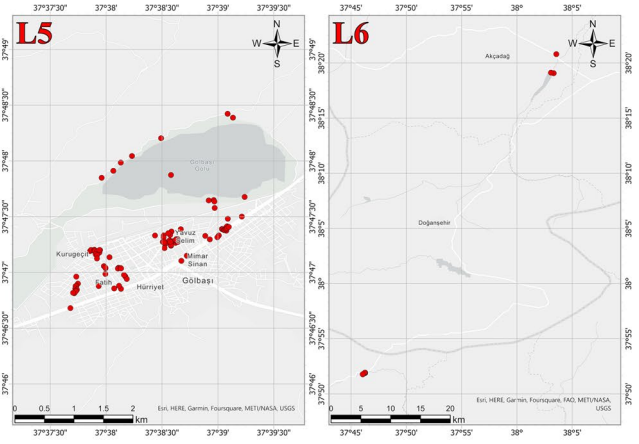

(a)

Excessive settlement, bearing capacity failures, soil ejecta at Lat:37.788˚N, Long:37.642˚E

Soil ejecta at Lat:37.78166˚N, Long:37.62913056˚E

(b)

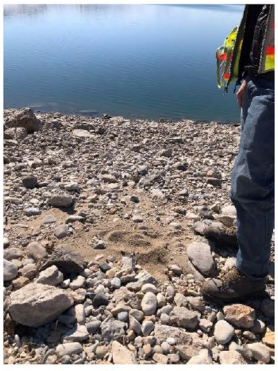

Sand boil at Lat: 38.31860˚N, Long: 38.05129˚E

Lateral spreading at Lat:38.34652˚N, Long: 38.0593˚E

(c)

Fig. 5 **a)** A higher resolution map of liquefaction regions L5 and L6, **b)** sample pictures from L5 region, and **c)** sample pictures from L6 region

Table 1 A sample summary of coordinates and liquefaction manifestation types of liquefaction sites

Site ID	Latitude (ºN)	Longitude (ºE)	Liquefaction manifestation	References
1	37.7862917	37.631728	Soil ejecta	Cetin and Ilgac (2003)
2	37.7827083	37.62888056	Lateral spreading	Cetin and Ilgac (2003)
.	.	.	.	.
.	.	.	.	.
.	.	.	.	.
427	37.33689	37.04538	SE	Cetin et al. (2023b)
428	37.33722	37.04549	SE	Cetin et al. (2023b)

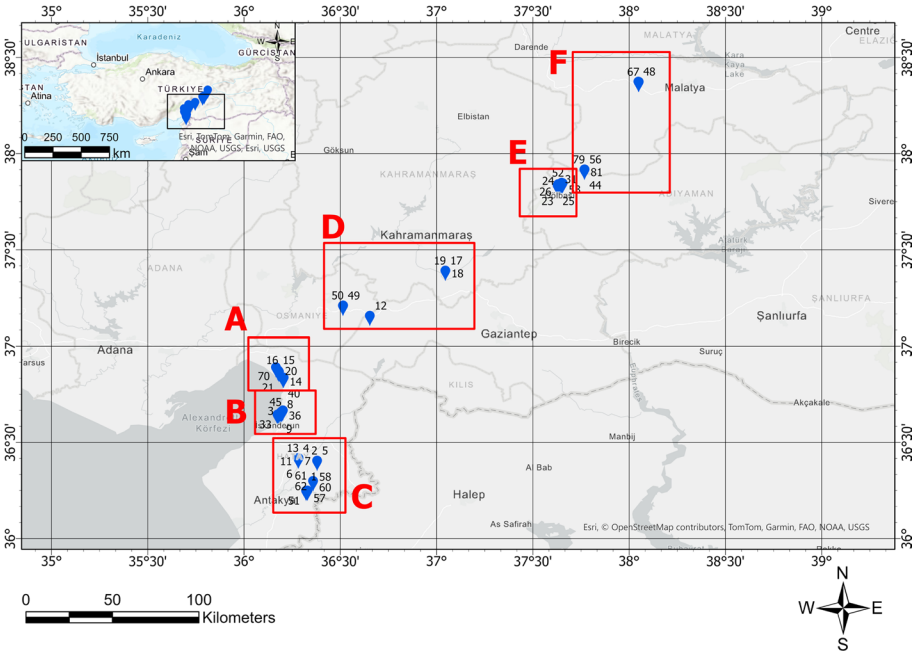

Fig. 6 The locations of sites where ejecta samples were collected

Ejecta samples after labeling were brought to METU Soil Mechanics Laboratory. They were oven dried for 24 h. After drying, a representative amount of sample portion was taken and put in sodium hexametaphosphate solution (5 ml/1000 g) overnight to ensure separation of soil particles. Following that, wet sieving is conducted to separate and collect the finer portion (< 0.074 mm) of the specimen. Fines portions is accumulated in large bottles for further grain size assessments. Coarser portions after the wet sieving are oven dried again, then tested for dry sieving. These abovementioned procedures are performed in conformance with ASTM International (2017) D6913, ASTM International (2016) D7928. The Atterberg limits of the retrieved samples are estimated

Fig. 7 A sample picture showing liquefied soil ejecta retrieved from six regions A through F

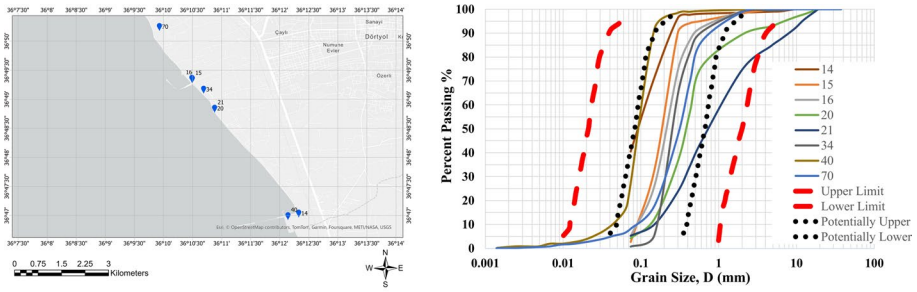

Fig. 8 **a)** Retrieved samples from Region A, **b)** the grain size distribution curves of the ejecta

Table 2 A summary of the site coordinates and soil classification characteristic of the ejecta samples from Region A

Sample ID #	Latitude (°)	Longitude (°)	Color	USCS soil type	Gravel content (%)	Sand content (%)	Fines content (%)	D_{10} (mm)	D_{30} (mm)	D_{60} (mm)	Liquid limit (%)	Plastic limit (%)	Plasticity index	Uniformity coefficient C_U	Coefficient of curvature C_C
14	36.782708	36.205458	Brown	SM	1.0	58.5	40.5	< 0.075	< 0.075	0.12	–	–	–	–	–
15	36.821216	36.174943	Dark brown	SP	0.3	97.0	2.7	0.09	0.15	0.21	–	–	–	2.3	1.2
16	36.821368	36.174806	Dark brown	SP	0.0	94.8	5.2	0.09	0.16	0.24	–	–	–	2.7	1.2
20	36.812778	36.181332	Black	SP	7.1	88.7	4.2	0.14	0.26	0.45	–	–	–	3.2	1.1
21	36.812778	36.181332	Black	SP	15.3	79.5	5.2	0.15	0.38	1.06	–	–	–	7.1	0.9
34	36.818233	36.178178	Black	SP	0.6	98.7	0.7	0.16	0.21	0.28	–	–	–	1.8	1.0
40	36.781958	36.202367	Gray	SM	0.0	72.8	27.2	< 0.075	0.08	0.11	NP			–	–
70	36.8362	36.1655	Gray	SM	0.0	91.8	8.2	< 0.075	0.21	0.38	NP			–	–

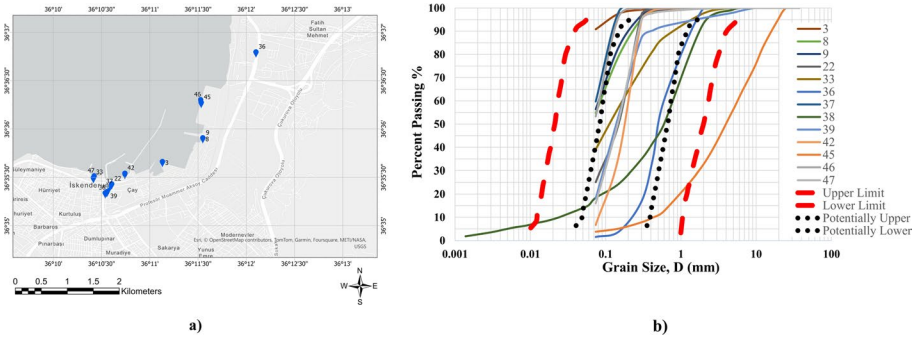

Fig. 9 **a)** Retrieved samples from Region B, **b)** the grain size distribution curves of the ejecta

as per ASTM D4318 (2010). Laboratory test results will be presented next, separately for each ejecta region.

4.1 Region A- Dörtyol, Hatay

Soil ejecta from 8 different locations were collected. 3 of them were sampled from industrial zones, whereas the rest were sampled from a shoreline and a port. The locations of these sites are shown in Fig. 8a. Similarly, Table 2 summarizes the coordinates of these sites along with the color of the ejecta and major soil classification test results. The samples from the shoreline were classified as clean sands with fines percent < 5–6%. The sample taken from the metallurgical facility with ID #40, is classified as non-plastic, and its fines and silt contents are estimated as 27.2 and 25%, respectively. The grain size distribution curves of soil ejecta are comparatively shown in Fig. 8b, along with liquefaction susceptibility bounds of Tschuida (1970). They are observed to consistently fall within the suggested susceptible soils range. A more comprehensive presentation of liquefaction triggering assessments for the soil ejecta sites, accompanied by the documentation of available borelogs and laboratory test results, can be found elsewhere (Cakir and Cetin 2024; Sahin and Cetin 2024). These details will not be reiterated herein.

4.2 Region B—Çay Neighborhood, İskenderun

In this region, a total of 13 soil ejecta samples were retrieved. 6 samples were collected from ports, while the remaining 7 were collected from the İskenderun-Çay neighborhood. The locations of these sites are shown in Fig. 9a. Coordinates of these sites, color of the soil ejecta as well as major soil classification test results are summarized in Table 3. All samples were classified as non-plastic. The sample retrieved from the Çay neighborhood with ID #38 has fines and silt contents of 18.4 and 15%, respectively. Figure 9b shows that except for the specimen ID #45, which has a gravel content of 45%, all grain size distribution curves of the ejecta material fall within the bounds of "susceptible to liquefaction region" defined by Tsuchida (1970). A more comprehensive presentation of liquefaction triggering assessments for the soil ejecta sites, accompanied by the documentation of available borelogs and laboratory test results, can be found elsewhere (Ozener et al. 2024; Bol et al. 2024). These details will not be reiterated herein.

Table 3 A summary of site coordinates and soil classification of the samples from Region B

Sample ID #	Latitude (°)	Longitude (°)	Color	USCS soil type	Gravel content (%)	Sand content (%)	Fines content (%)	D_{10} (mm)	D_{30} (mm)	D_{60} (mm)	Liquid limit (%)	Plastic limit (%)	Plasticity index	Uniformity coefficient C_U	Coefficient of curvature C_C
3	36.593344	36.185508	Gray	ML	0.0	9.1	90.9	< 0.075	< 0.075	< 0.075	NP			–	–
8	36.597441	36.192487	Black	ML	0.0	45.2	54.8	< 0.075	< 0.075	0.08	NP			–	–
9	36.597441	36.192487	Black	-	0.1	43.4	56.4	< 0.075	< 0.075	0.08	–	–	–	–	–
22	36.589542	36.176742	Black	SM	0.0	74.9	25.1	< 0.075	0.09	0.18	NP			–	–
33	36.590614	36.173581	Black	-	0.0	60.9	39.1	< 0.075	< 0.075	0.17	–	–	–	–	–
36	36.612282	36.201672	Black	SP	0.0	98.5	1.5	0.23	0.40	0.60	–	–	–	2.6	1.2
37	36.589053	36.176361	Black	ML	0.0	40.2	59.8	< 0.075	< 0.075	0.08	NP			–	–
38	36.587997	36.175633	Gray	SM	0.9	80.7	18.4	< 0.075	0.22	0.80	NP			–	–
39	36.588200	36.175922	Black	-	2.1	79.8	18.1	< 0.075	0.09	0.17	–	–	–	–	–
42	36.591317	36.179025	Black	SP	0.0	93.3	6.7	0.08	0.14	0.20	–	–	–	2.5	1.2
45	36.603550	36.192210	Gray	SW	44.9	51.3	3.8	0.45	1.80	5.70	–	–	–	12.7	1.3
46	36.604020	36.192110	Gray	ML	0.0	46.7	53.3	< 0.075	< 0.075	0.08	NP			–	–
47	36.590870	36.173710	Gray	SM	0.0	84.0	16.0	< 0.075	0.10	0.17	NP			–	–

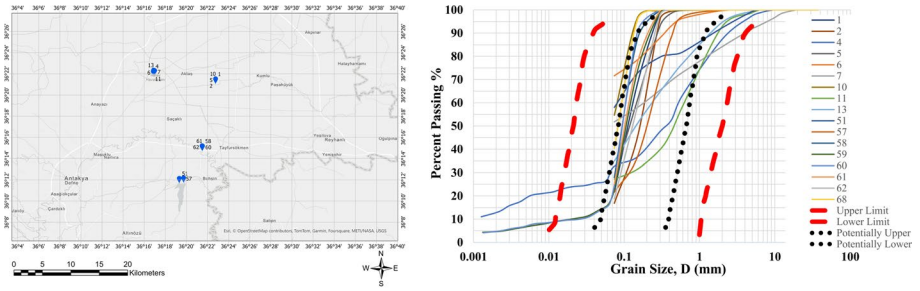

Fig. 10 **a)** Retrieved samples from Region C, **b)** the grain size distribution curves of the ejecta

4.3 Region C—Hatay Airport, Demirköprü Bridge, Yarseli Dam, Tepehan Village

In this relatively wide region, a total of 17 samples were retrieved: 5 samples were collected from Hatay Airport (#4,6,7,11,13), 6 samples were from a site in the proximity of Demirköprü Bridge, which was severely damaged due to soil liquefaction (#58,59,60,61,62,68), 2 samples were taken from Yarseli Dam site (#51,57), and remaining 4 were sampled from a farmland (#1,2,5,10) in Tepehan village. For the Demirköprü Bridge site, the retrieved non plastic ejecta sample has 25% fines contents, in the average. Ejecta samples collected from the farmland are also non plastic. On the contrary, samples retrieved from Hatay airport have plasticity index values varying in between 21 to 37. In the same region, one of the samples from Yarseli Dam (#57) has 58% fines content with plasticity index of 28. The geographical positions of these sites are shown in Fig. 10a, and grain size distribution of the ejecta are shown in Fig. 10b. Further details, including the coordinates of these sites, the color of the soil ejecta, and the major soil classification test results are summarized in Table 4. A more comprehensive presentation of liquefaction triggering assessments for the soil ejecta sites, accompanied by the documentation of available borelogs and laboratory test results, can be found elsewhere (Cetin et al. 2024a, 2024b; Ocak and Cetin 2024; Bol et al. 2024). These details will not be reiterated herein.

4.4 Region D—Gaziantep

Four of the samples in this region were retrieved from a farmland, and the remaining two were sampled from the Arıklıkaş Dam site. Figure 11a displays the site locations. The coordinates of these sites, the color of the ejecta, and the main soil classification test results are summarized in Table 5. Only one specimen (ID #49) is categorized as low plasticity clay (CL), while the others are classed as silty sand (SM) or clayey sand (SC). Figure 11b illustrates the grain size distribution curves of the soil ejecta, which fall within the Tsuchida (1970) liquefaction susceptibility bounds.

4.5 Region E—Gölbaşı, Adıyaman

Due to the high number of residential buildings where foundation failures due to liquefaction induced bearing capacity failures, excessive settlements and lateral spreading, the

Table 4 A summary of site coordinates and soil classification of the samples from Region C

Sample ID #	Latitude (°)	Longitude (°)	Color	USCS soil type	Gravel content (%)	Sand content (%)	Fines content (%)	D_{10} (mm)	D_{30} (mm)	D_{60} (mm)	LL (%)	PL (%)	Plasticity index	Uniformity coefficient C_U	Coefficient of curvature C_C
1	36.350516	36.379327	Light brown	SC or SM	0.0	78.3	21.7	< 0.075	0.09	0.13	–	–	–	–	–
2	36.350916	36.379327	Light brown	SC or SM	0.0	83.2	16.8	< 0.075	0.11	0.19	–	–	–	–	–
4	36.362648	36.280920	Light brown	SC	3.0	64.2	32.8	< 0.075	0.07	0.53	32	11	21	–	–
5	36.350916	36.379327	Brown	SM	0.0	72.2	27.8	< 0.075	0.08	0.15	NP			–	–
6	36.362648	36.280920	Light brown	CH	0.0	28.4	71.6	< 0.075	< 0.075	< 0.075	56	20	36	–	–
7	36.363890	36.283064	Brown	CL	8.5	39.7	51.8	< 0.075	< 0.075	0.19	48	17	31	–	–
10	36.350916	36.379327	Brown	ML	0.0	45.3	54.7	< 0.075	< 0.075	0.08	NP			–	–
11	36.362648	36.280920	Light brown	SC	1.5	71.3	27.2	< 0.075	0.13	0.64	30	11	19	–	–
13	36.364562	36.281468	Light brown	SC or SM	0.7	64.4	34.9	< 0.075	< 0.075	0.24	–	–	–	–	–
51	36.194480	36.321980	Grayish brown	CL	1.0	41.0	58.0	< 0.075	< 0.075	0.08	44	16	28	–	–
57	36.195355	36.328872	Yellowish brown	SC or SM	0.0	78.4	21.6	< 0.075	0.12	0.24	–	–	–	–	–
58	36.2451	36.35865	Light brown	SM	0.0	72.0	28.0	< 0.075	0.08	0.11	NP			–	–
59	36.24509	36.35864	Brown	SM	0.0	77.3	22.7	< 0.075	0.09	0.12	NP			–	–
60	36.24507	36.35866	Light brown	SM	0.0	75.2	24.8	< 0.075	0.08	0.11	NP			–	–
61	36.24506	36.3581	Light brown	SC or SM	0.0	74.9	25.1	< 0.075	0.08	0.12	–	–	–	–	–
62	36.24527	36.35794	Light brown	SM	0.0	81.2	18.8	< 0.075	0.09	0.16	NP			–	–
68	36.245145	36.357975	Brown	SM	0.0	59.6	40.4	< 0.075	< 0.075	0.09	NP			–	–

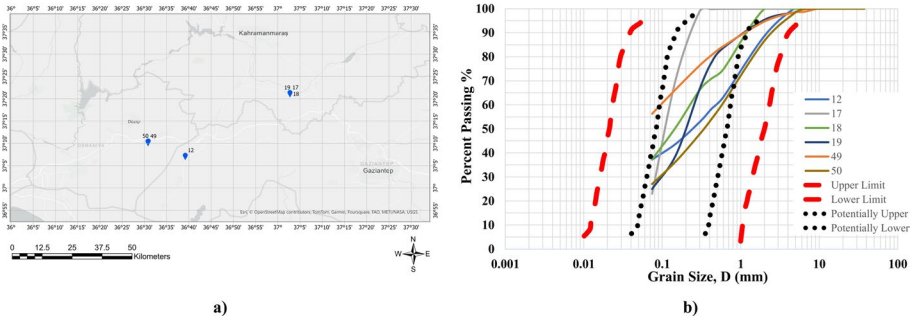

Fig. 11 **a)** Retrieved samples from Region D, **b)** the grain size distribution curves of the ejecta

highest number of specimens (31 samples) were collected from Gölbaşı-Adıyaman as shown in Fig. 12a. All samples were brown in color. Out of 20 samples, for which Atterberg limit tests were performed, 19 of them have plasticity index values varying in the range of 16 to 23%, except for sample #76, which has a plasticity index of 34%. These soil classification test results will be further elaborated as part of susceptibility of fines containing soil mixtures discussions. Figure 12b illustrates the grain size distribution curves of the soil ejecta. Large number of ejecta grain size distribution curves fall outside the liquefaction susceptibility limits defined by Tsuchida (1970) due to their high fines content. Out of 31 specimens, hydrometer tests were performed on 6 to estimate their clay contents. Clay contents of these 6 samples were estimated to vary in the range of 13–20%. Further details, including the coordinates of these sites, the color of the soil ejecta, and the major soil classification test results are summarized in Table 6. A more comprehensive presentation of liquefaction triggering assessments for the soil ejecta sites, accompanied by the documentation of available borelogs and laboratory test results, can be found elsewhere (Cetin et al. 2024c). These details will not be reiterated herein.

4.6 Region F—Doğanşehir, Malatya

6 samples were collected from this region. Two of them (ID #48 and 67) were sampled from Sultansuyu Dam, located on Sultansuyu River in Malatya. The other 4 ejecta samples (#44,56,79,81) were retrieved along the benches of Goksu Stream, next to a liquefaction-induced retaining wall failure. The geographic positions of these ejecta are presented in Fig. 13a. Table 7 provides a summary of site coordinates, the color of the soil ejecta, and major soil classification test results. Out of 4 samples from the failed retaining wall, 2 of them were classified as non-plastic. The grain size distribution curves of the soil ejecta are comparatively shown in Fig. 13b, which consistently fall within the liquefaction susceptibility bounds of Tsuchida (1970) except for the sample #67, which is retrieved from Sultansuyu Dam site, and classified as silty, clayey gravel (GM or GC). A more comprehensive presentation of liquefaction triggering assessments for the soil ejecta sites, accompanied by the documentation of available borelogs and laboratory test results, can be found elsewhere (Cetin et al. 2024d). These details will not be reiterated herein.

Table 5 A summary of site coordinates and soil classification of the samples from Region D

Sample ID #	Latitude (°)	Longitude (°)	Color	USCS soil type	Gravel content (%)	Sand content (%)	Fines content (%)	D_{10} (mm)	D_{30} (mm)	D_{60} (mm)	Liquid limit (%)	Plastic limit (%)	Plasticity index	Uniformity coefficient C_U	Coefficient of curvature C_C
12	37.102448	36.653048	Brown	SC or SM	0.0	62.8	37.2	< 0.075	< 0.075	0.49	–	–	–	–	–
17	37.337169	37.045456	Brown	SM	0.0	77.0	23.0	< 0.075	0.08	0.13	NP			–	–
18	37.337044	37.045609	Gray	SC	0.0	62.7	37.3	< 0.075	< 0.075	0.23	34	13	21	–	–
19	37.337044	37.045609	Gray	SC or SM	1.6	73.5	25.0	< 0.075	0.10	0.26	–	–	–	–	–
49	37.155110	36.513110	Gray	CL	1.6	42.1	56.3	< 0.075	< 0.075	0.10	41	16	25	–	–
50	37.155890	36.514400	Black	SC	2.0	71.0	27.0	< 0.075	0.09	0.60	32	12	20	–	–

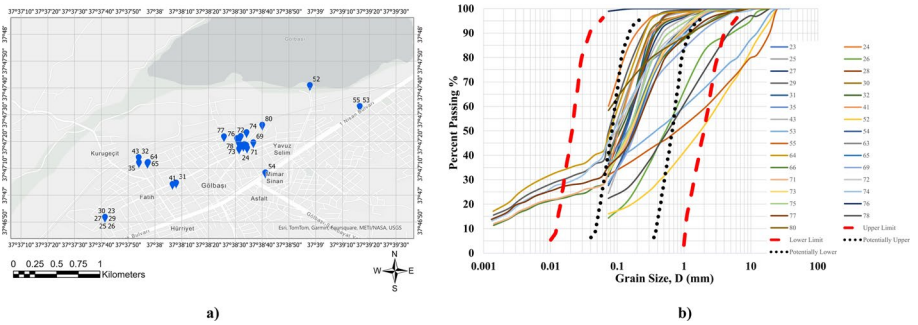

Fig. 12 **a)** Retrieved samples from Region E, **b)** the grain size distribution curves of the ejecta

5 Liquefaction susceptibility of fines containing soil mixtures

Laboratory test results, performed on liquefied soil ejecta, are shown on the plasticity chart shown in Fig. 14. The liquefied ejecta samples are mostly classified as low plasticity clays (CL). Most of this CL type soil ejecta are retrieved from Gölbaşı-Adıyaman region. The liquid limits of these samples vary in between 32 and 38%. Their plasticity index values are estimated to be in the range of 16 to 23%. Unexpectedly, two ejecta samples with plasticity indices higher than 30% are retrieved from Hatay airport, one of which is classified as high plasticity clay (CH).

Laboratory test results are also comparatively shown on the Seed et al. (2003) liquefaction susceptibility chart, given in Fig. 15. The majority of the ejecta samples fall on "Zone B: Testing Recommended" region of the chart. However, inconsistently, 12 out of 74 samples fall outside the susceptibility region of the Seed et al. chart.

Finally, laboratory test results are jointly presented along with the Wang (1979) data, which were compiled from samples of liquefied "silty soil" layers at 7 sites in China. Figure 16 presents comparatively the overall database on the plasticity chart, which clearly suggests that clayey soils are liquefiable and capable of producing ejecta when subjected to strong cyclic loading. Detailed site investigation and laboratory testing programs are ongoing to investigate the liquefaction (cyclic) responses of fine-grained soils liquefied during Türkiye-Kahramanmaraş earthquake sequence. Their results are believed to contribute to current state of knowledge and practice on assessing cyclic response of fine-grained soils. Until the findings of these studies become available, the liquefaction susceptibility of silty-clayey soils mixtures is recommended to be assessed cautiously and conservatively.

6 Summary and conclusions

Seismically induced soil liquefaction was listed as one of the major sources of damage observed in the natural and built environment during the 2023 Kahramanmaraş earthquake sequence. After the earthquakes, reconnaissance field investigations were performed to collect perishable data and document the extent of damage. As part of these reconnaissance

Table 6 A summary of site coordinates and soil classification of the samples from Region E

Sample ID #	Latitude (°)	Longitude (°)	Color	USCS soil type	Gravel content (%)	Sand content (%)	Fines content (%)	D_{10} (mm)	D_{30} (mm)	D_{60} (mm)	LL (%)	PL (%)	PI	Uniformity coefficient C_U	Coefficient of curvature C_C
23	37.780461	37.628144	Dark brown	SM or SC	0.0	67.1	32.9	< 0.075	< 0.075	0.18	–	–	–	–	–
24	37.787536	37.642056	Dark brown	CL or CH or ML or MH	0.0	39.9	60.1	< 0.075	< 0.075	< 0.075	–	–	–	–	–
25	37.780461	37.628144	Brown	SC	0.0	56.2	43.8	< 0.075	< 0.075	0.12	35	13	22	–	–
26	37.780461	37.628144	Brown	SM	10.7	74.9	14.4	< 0.075	0.23	0.80	NP			–	–
27	37.780461	37.628144	Brown	SM or SC	0.0	63.6	36.4	< 0.075	< 0.075	0.18	–	–	–	–	–
28	37.780461	37.628144	Brown	SC	0.0	64.7	35.3	< 0.075	< 0.075	0.17	32	14	18	–	–
29	37.780461	37.628144	Brown	SC	0.0	50.5	49.5	< 0.075	< 0.075	0.10	37	17	20	–	–
30	37.780461	37.628144	Brown	SM or SC	0.0	62.1	37.9	< 0.075	< 0.075	0.13	–	–	–	–	–
31	37.784008	37.635528	Brown	SM or SC	0.0	68.6	31.4	< 0.075	< 0.075	0.17	–	–	–	–	–
32	37.786644	37.631642	Brown	SM or SC	0.0	59.9	40.1	< 0.075	< 0.075	0.16	–	–	–	–	–
35	37.786111	37.631667	Brown	SC	0.0	61.5	38.5	< 0.075	< 0.075	0.21	35	19	16	–	–
41	37.783867	37.635150	Brown	SM or SC	0.0	66.2	33.8	< 0.075	< 0.075	0.13	–	–	–	–	–
43	37.786644	37.631642	Brown	SC	0.0	75.5	24.5	< 0.075	0.09	0.20	33	17	16	–	–
52	37.79411	37.64940	Brown	SM or SC	32.1	51.9	16.0	< 0.075	0.46	3.20	–	–	–	–	–
53	37.79194	37.65457	Brown	SC	22.3	40.5	37.2	< 0.075	< 0.075	1.10	35	16	19	–	–
54	37.78506	37.64478	Brown	SC	0.0	72.3	27.7	< 0.075	0.08	0.24	36	17	19	–	–
55	37.79194	37.65457	Brown	SM or SC	29.9	38.1	32.0	< 0.075	< 0.075	2.20	–	–	–	–	–

Table 6 (continued)

Sample ID #	Latitude (°)	Longitude (°)	Color	USCS soil type	Gravel content (%)	Sand content (%)	Fines content (%)	D_{10} (mm)	D_{30} (mm)	D_{60} (mm)	LL (%)	PL (%)	PI	Uniformity coefficient C_U	Coefficient of curvature C_C
63	37.787817	37.642496	Brown	SC	0.0	59.2	40.8	< 0.075	< 0.075	0.15	33	17	16	–	–
64	37.78606	37.632548	Brown	SC	0.9	50.9	48.1	< 0.075	< 0.075	0.11	36	18	18	–	–
65	37.786139	37.632603	Brown	SC	0.0	71.6	28.4	< 0.075	0.08	0.24	35	17	18	–	–
66	37.787907	37.642796	Brown	SC	1.2	66.2	32.6	< 0.075	< 0.075	0.22	36	16	20	–	–
69	37.788182	37.643535	Brown	SM or SC	2.2	69.0	28.9	< 0.075	0.08	0.25	–	–	–	–	–
71	37.78763	37.64288	Brown	SC	0.0	66.6	33.4	< 0.075	< 0.075	0.23	35	15	20	–	–
72	37.78883	37.642225	Brown	SC	0.0	55.7	44.3	< 0.075	< 0.075	0.15	36	16	20	–	–
73	37.78811	37.64204	Brown	SC	0.0	67.0	33.0	< 0.075	< 0.075	0.22	32	16	16	–	–
74	37.78923	37.64283	Brown	SC	2.1	52.0	45.8	< 0.075	0.02	0.14	35	16	19	–	–
75	37.78801	37.6426	Brown	SC	0.0	66.0	34.0	< 0.075	< 0.075	0.20	33	16	17	–	–
76	37.78844	37.64191	Brown	CH	0.0	1.0	99.0	< 0.075	< 0.075	< 0.075	54	20	34	–	–
77	37.7888	37.64049	Brown	SC	1.4	63.2	35.4	< 0.075	0.05	0.26	35	16	19	–	–
78	37.78861	37.64185	Brown	SC	9.7	67.9	22.4	< 0.075	0.19	0.95	32	15	17	–	–
80	37.79	37.64446	Brown	CL	1.8	39.8	58.4	< 0.075	< 0.075	0.08	42	19	23	–	–

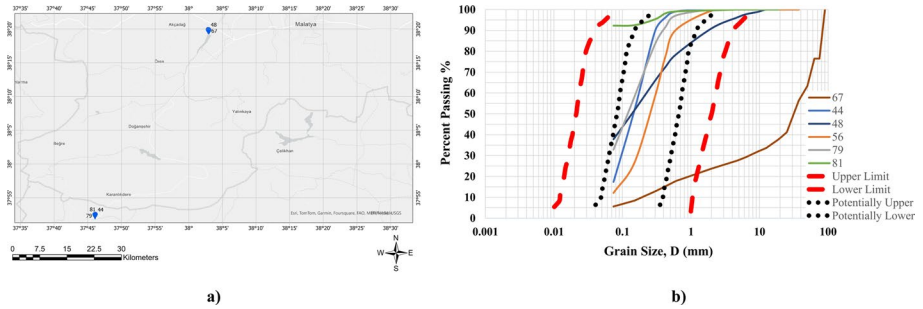

Fig. 13 **a)** Retrieved samples from Region F, **b)** grain size distribution curves of the ejecta

studies, the sites with surface manifestations of seismic soil liquefaction in the form of soil ejecta, excessive foundation and ground deformations were identified and documented. The deformations were mapped and samples from ejecta, if available, were retrieved. Within the scope of this manuscript, the liquefied soil sites were introduced. The results of soil classification tests, performed on the retrieved soil ejecta at liquefied sites, were comparatively shown on the liquefaction susceptibility chart of Seed et al. (2003). Additionally, the soil liquefaction database of Wang (1979), composed of fine grained soils, is also used in the comparisons.

The majority of the ejecta samples were classified as sands with varying degrees of fines. Laboratory test results revealed that fines-containing liquefied ejecta samples were mostly classified as low plasticity clays (CL). Most of these CL type soil ejecta samples were retrieved from Gölbaşı-Adıyaman region. The liquid limits of these samples varied in between 32 to 38%. Their plasticity index values were estimated to be in the range of 16 to 23%. Surprisingly, two ejecta samples with plasticity indices higher than 30% were retrieved from Hatay airport, one of which was classified as high plasticity clay (CH). The majority of the fine-grained ejecta samples fall on "Zone B: Testing Recommended" region of the Seed et al. (2003) susceptibility chart. Unexpectedly, 12 out of 74 samples fall outside the susceptible limits of Seed et al. The laboratory testing of soil ejecta retrieved after Türkiye-Kahramanmaraş earthquake sequence prematurely suggested that clayey soils are capable of producing ejecta when subjected to cyclic loading. Detailed site investigation and laboratory testing programs are ongoing to further investigate this rather unexpected response. The results of these ongoing research studies are believed to provide further input to seismically induced liquefaction response of fine-grained soils. Until they become available, the liquefaction susceptibility of silty-clayey soils mixtures is recommended to be assessed conservatively with caution.

Table 7 A summary of site coordinates and soil classification of the samples from Region F

Sample ID #	Latitude (°)	Longitude (°)	Color	USCS soil type	Gravel content (%)	Sand content (%)	Fines content (%)	D_{10} (mm)	D_{30} (mm)	D_{60} (mm)	Liquid limit (%)	Plastic limit (%)	Plasticity index	Uniformity coefficient C_U	Coefficient of curvature C_C
44	37.86296	37.767700	Grayish brown	SM	0.0	82.6	17.4	< 0.075	0.10	0.18	NP			–	–
48	38.31954	38.047920	Light brown	SM or SC	3.7	58.4	37.9	< 0.075	< 0.075	0.23	–	–	–	–	–
56	37.86301	37.76788	Gray	SM or SC	0.0	87.9	12.1	< 0.075	< 0.075	0.08	–	–	–	–	–
67	38.31871	38.050074	Grayish brown	GM or GC	72.4	22.0	5.6	0.20	7.50	44.00	–	–	–	220.0	6.4
79	37.863	37.76739	Gray	SM	0.0	67.1	32.9	< 0.075	< 0.075	0.16	NP			–	–
81	37.86336	37.76862	Gray	CL	0.0	7.7	92.3	< 0.075	< 0.075	< 0.075	29	16	13	–	–

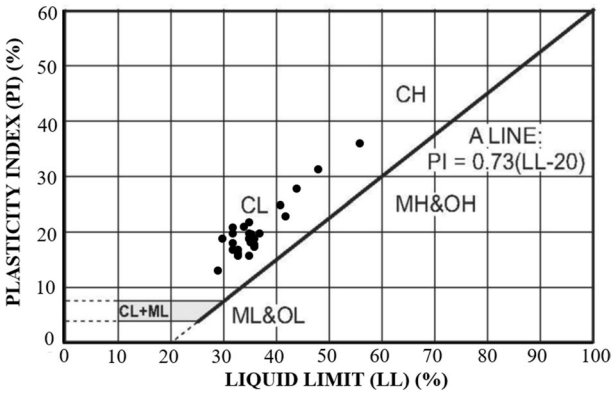

Fig. 14 Fine-grained ejecta shown on the plasticity chart

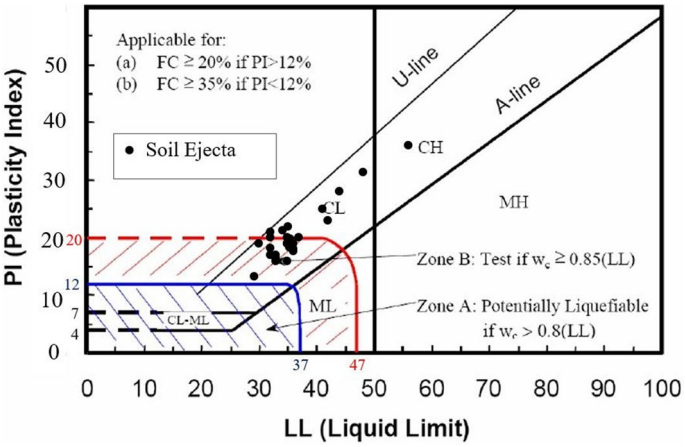

Fig. 15 Liquefaction Susceptibility Assessment of Fines Containing Soil Ejecta by Seed et al. (2003)

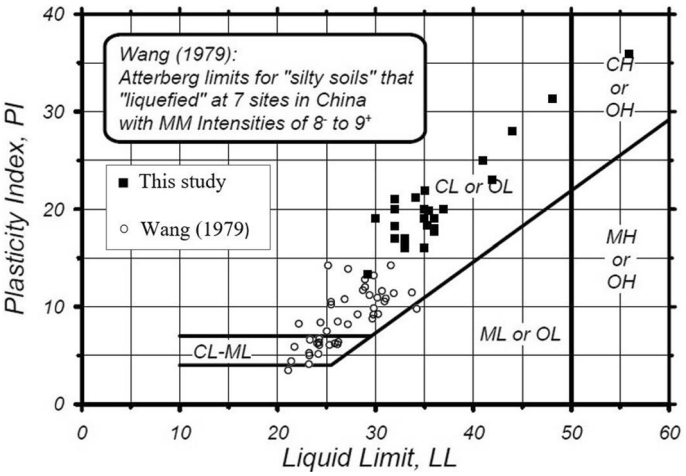

Fig. 16 Assessment of liquefiable soil types by Wang (1979) (after Boulanger 2004)

Supplementary Information The online version contains supplementary material available at https://doi.org/10.1007/s10518-024-01875-3.

Acknowledgements We would like to acknowledge the partial funding provided for the fieldwork by The Scientific and Technological Research Institution of Turkiye (TÜBİTAK) "1002-C Natural Disasters-Focused Fieldwork Emergency Support Program (Doğal Afetler Odaklı Saha Çalışması Acil Destek Programı)".

Author contributions Material preparation, data collection and analyses were performed by Kemal Onder Cetin, Berkan Soylemez, Hayri Güzel and Elife Cakir. The manuscript was drafted by Kemal Onder Cetin, and all authors commented on the draft. All authors read and approved the final version of the manuscript.

Funding Open access funding provided by the Scientific and Technological Research Council of Türkiye (TÜBİTAK). This work is partially supported by The Scientific and Technological Research Institution of Turkiye (TÜBİTAK) "1002-C Natural Disasters-Focused Fieldwork Emergency Support Program (Doğal Afetler Odaklı Saha Çalışması Acil Destek Programı)".

Data availability The datasets generated during and/or analyzed during the current study are available in the provided references and can also be provided by the corresponding author upon reasonable request.

Declarations

Competing interests The authors have no relevant financial or non-financial interests to disclose.

References

ASTM D4318-10e1 (2010) Standard test methods for liquid limit, plastic limit, and plasticity index of soils. ASTM International, West Conshohocken, PA

ASTM International (2016) D7928-17 Standard test method for particle-size distribution (gradation) of fine-grained soil using the sedimentation (hydrometer) analysis. West Conshohocken, PA

ASTM International (2017) D6913/D6319M-17 standard test method for particle-size distribution (gradation) of soils using sieve analysis. West Conshohocken, PA

Bol E, Özocak A, Sert S, Cetin KO, Arslan E, Kocaman K, Ayhan BU (2024) Evaluation of soil liquefaction in the City of Hatay Triggered After the February 6, 2023 Kahramanmaraş-Türkiye Earthquake Sequence

Boulanger RW, Idriss IM (2004) Evaluating the potential for liquefaction or cyclic failure of silts and clays (p. 131). Davis, California: Center for Geotechnical Modeling

Çakir E, Cetin KO (2024) Liquefaction triggering and induced ground deformations at a metallurgical facility in Dörtyol-Hatay after the February 6 Kahramanmaraş Earthquake Sequence—Soil Dynamics and Earthquake Engineering

Cetin KO, Ilgac M (2023) Reconnaissance report on February 6, 2023 Kahramanmaraş-Pazarcık (M_w=7.7) and Elbistan (M_w=7.6) Earthquakes. Türkiye Earthquake Reconnaissance and Research Alliance. https://doi.org/10.13140/RG.2.2.15569.61283/1

Cetin KO, Bray JD, Frost JD, Hortacsu A, Miranda E, Moss RES, Stewart JP (2023a) February 6, 2023, Türkiye Earthquakes: report on geoscience and engineering impacts. Geotechnical Extreme Event Reconnaissance Association (GEER), the Earthquake Engineering Research Institute, and the Earthquake Engineering Foundation of Türkiye. GEER Association Report 082. https://doi.org/10.18118/G6PM34

Cetin KO, Ilgac M, Can G, and Çakır E (2023b) Preliminary reconnaissance report on February 6, 2023, Pazarcık M_w=7.7 and Elbistan Mw=7.6, Kahramanmaraş-Türkiye Earthquakes. Middle East Technical University Earthquake Engineering Research Center (METU EERC) Report No: METU/EERC 2023-01. https://doi.org/10.13140/RG.2.2.32975.97446

Cetin KO, Cakir E, Eyigün Y, Gökçeoğlu C (2024a) soil liquefaction manifestations at Hatay Airport after the February 2023 Türkiye Earthquake Sequence-EQSpectra

Cetin KO, Cüceoğlu F, Yildirim S, Ayhan BU, Aydin S (2024b) Performance of Yarseli Dam During February 6, 2023, Kahramanmaraş-Türkiye Earthquake Sequence –Journal of Erathquake Engineering

Cetin KO, Moug D, Soylemez B, Ayhan BU, Zarzour M, Suhaily AA, Akil B, Unutmaz B, Firat S, Tekin E, Cakir E, Frost D, Macedo J, Bray J, Moss R, Bassal P, Gurbuz A, Işık NS, Akin M, Sahin A, Duman E (2024c) Ground failures and foundation performances in Adıyaman-Gölbaşı -EQSpectra

Cetin KO, Yildirim S, Demirdöğen S, Cüceoğlu F, Ayhan BU (2024d) Performance of Sultansuyu Dam During February 6, 2023, Türkiye-Kahramanmaraş Earthquake Sequence—Bulletin of Earthquake Engineering

Moug D, Bassal P, Bray JB, Cetin KO, Kendir SB, Şahin A, Çakır E, Söylemez B, and Ocak S (2023) February 6, 2023, Türkiye Earthquakes: GEER Phase 3 team report on selected geotechnical engineering effects. Geotechnical Extreme Event Reconnaissance Association, GEER Association Report 082-S1. https://doi.org/10.18118/G6F379

Ocak S, Cetin KO (2024) Liquefaction-induced failure of Demirköprü Bridge Pile Foundation and Retaining System Following the February 6 Kahramanmaraş Earthquake Sequence—Journal of Earthquake Engineering

Özener P, Monkul MM, Bayat EE, Ari A, Cetin KO (2024) Liquefaction and performance of foundation systems in Iskenderun during 2023 Kahramanmaras-Turkiye Earthquake Sequence—Soil dynamics and Earthquake Engineering

Sahin A, Cetin KO (2024) The assessment of soil liquefaction triggering performances at two petrochemical facilities following the February 6, 2023, Kahramanmaras Earthquake Sequence—Engineering Geology

Seed RB, Cetin KO, Moss RES, Kammerer A, Wu J, Pestana J, Riemer M, Sancio RB, Bray JD, Kayen RE, Faris A (2003) Recent advances in soil liquefaction engineering: a unified and consistent framework. Keynote presentation, 26th Annual ASCE Los Angeles Geotechnical Spring Seminar, Long Beach, CA

Tsuchida H (1970) Prediction and countermeasure against the liquefaction in sand deposits. Abstract of the Seminar in the Port and Harbor Research Institute (in Japanese)

Wang, W (1979) Some findings in soil liquefaction, Water Conservancy and Hydroelectric Power Scientific Research Institute, Beijing, China